The Siderocalin/Enterobactin Interaction: A Link between Mammalian Immunity and Bacterial Iron Transport[1]

Rebecca J. Abergel,[†] Matthew C. Clifton,[§] Juan C. Pizarro,[§] Jeffrey A. Warner,[‡] David K. Shuh,[‡,] Roland K. Strong,[§,]* and Kenneth N. Raymond[†,‡,]**

Contribution from the Department of Chemistry, University of California, Berkeley, CA 94720-1460, the Division of Basic Sciences, Fred Hutchinson Cancer Research Center, Seattle, WA 98109 and the Chemical Sciences Division, Lawrence Berkeley National Laboratory, Berkeley, CA 94720

raymond@socrates.berkeley.edu

[†]University of California, Berkeley

[§]Fred Hutchinson Cancer Research Center

[‡]Lawrence Berkeley National Laboratory

ABSTRACT: The siderophore enterobactin (Ent) is produced by enteric bacteria to mediate iron uptake. Ent scavenges iron and is taken up by the bacteria as the highly stable ferric complex $[Fe^{III}(Ent)]^{3-}$. This complex is also a specific target of the mammalian innate immune system protein, Siderocalin (Scn), which acts as an anti-bacterial agent by specifically sequestering siderophores and their ferric complexes during infection. Recent literature suggesting that Scn may also be involved in cellular iron transport has increased the importance of understanding the mechanism of siderophore interception and clearance by Scn; Scn is observed to release iron in acidic endosomes and $[Fe^{III}(Ent)]^{3-}$ is known to undergo a change from catecholate to salicylate coordination in acidic conditions, which is predicted to be sterically incompatible with the Scn binding pocket (also referred to as the calyx). To investigate the interactions between the ferric Ent complex and Scn at different pH values, two recombinant forms of Scn with mutations in three residues lining the calyx were prepared: Scn-W79A/R81A and Scn-Y106F. Binding studies and crystal structures of the Scn-W79A/R81A:$[Fe^{III}(Ent)]^{3-}$ and Scn-Y106F:$[Fe^{III}(Ent)]^{3-}$ complexes confirm that such mutations do not affect the overall conformation of the protein but do weaken significantly its affinity for $[Fe^{III}(Ent)]^{3-}$. Fluorescence, UV-Vis and EXAFS spectroscopies were used to determine Scn/siderophore dissociation constants and to characterize the coordination mode of iron over a wide pH range, in the presence of both mutant proteins and synthetic salicylate analogs of Ent. While Scn binding hinders salicylate coordination transformation, strong acidification results in the release of iron and degraded siderophore. Iron release may therefore result from a combination of Ent degradation and coordination change.

Introduction

Withholding essential iron from infecting bacteria has long been known to be a key host defense mechanism.[2] A general bacteriostatic response is to upregulate expression of transferrin, lactoferrin receptors and ferritin, decreasing the concentration of extracellular iron in serum.[3] However, a more specific strategy involves the mammalian protein Siderocalin (Scn), also known as Lcn2, neutrophil-gelatinase-associated lipocalin, 24p3 or uterocalin.[4-6] Constitutively present in neutrophil granules, Scn is induced and secreted in response to activation of innate immune receptors, such as Toll-like receptor 4, in various cell types.[5] Scn complements the general anti-bacterial iron-depletion defense by specifically binding to bacterial ferric and apo siderophores, preventing significant early bacteraemia, while successful pathogens produce alternate or modified siderophores not bound by Scn to evade this defense.[7-9] The archetypical 2,3-catecholate siderophore enterobactin (Ent) is produced by numerous microorganisms and was the first identified target of Scn (Fig. 1).[6] The protein acts as a growth inhibitor of pathogens that rely solely on Ent-mediated iron acquisition by binding and sequestering the ferric siderophore complex, with an affinity for $[Fe^{III}(Ent)]^{3-}$ comparable to that of its cognate outer membrane receptor in *Escherichia coli*, FepA.[10] While other host iron-binding proteins chelate iron directly, Scn is unique in that it is specific for iron destined for bacterial use as a ferric siderophore complex and does not bind iron directly.

In addition to its role in innate immunity, Scn was also reported to be involved in kidney development as an iron-donating molecule[11], delivering iron to the cytoplasm, where it may activate or repress iron-responsive genes.[12] Therefore, Scn may be an alternative to transferrin in iron transport, important for tissue and organ development, possibly functioning at a point in development before circulation of transferrin and expression of transferrin receptors are established.[13] While the Scn iron unloading process depends on the cycling of the protein through acidic endosomes, similar to the transferrin iron delivery pathway, the pH sensitivity and subcellular targeting of Scn differ from those of transferrin.[12] Furthermore, a growing literature suggests that Scn is involved in apoptosis, possibly functioning by delivering or withdrawing iron from cells.[14] Subsequent studies have proposed that a putative mammalian siderophore is available to mediate iron transport and that Scn is recycled after delivering iron.[15,16] However, no mammalian siderophore has yet been identified and Scn loaded with $[Fe^{III}(Ent)]^{3-}$ was used as a surrogate to investigate the process of iron uptake and release in mammalian cells. If the strong binding of Scn to ferric-siderophore complexes is the key process for the protein to fulfill its pleiotropic physiological functions, then how is iron released from Scn? How does the interaction between Scn and $[Fe^{III}(Ent)]^{3-}$ participate in iron intracellular delivery?

The crystal structure of the Scn:$[Fe^{III}(Ent)]^{3-}$ complex shows that the protein binds the ferric-siderophore complex by intercalating the positively charged side chains of three residues (R81, K125 and K134) between the ligand catechol rings, each of which sits in a distinct sub-pocket of the trilobate calyx (Fig. 1).[6] These three residues form cyclically-permuted, hybrid electrostatic/cation-π interactions with $[Fe^{III}(Ent)]^{3-}$. Other key interactions are the hydrogen bonds formed between Y106 and the *meta*-phenolate oxygen of one Ent catecholate ring (in the first pocket between K134 and K125), herringbone-type interactions between ligand catechols and the side-chain of W79 (Fig. S1), and additional cation-π interactions between siderophore catechols and the side-chain of R81. The calyx is relatively rigid overall, with only the side chains of two residues, W79 and R81, showing any conformational variation in response to ligand binding.[6] While the metal-coordination chemistry of Ent has been studied extensively and its solution behavior is known to vary considerably with pH, the effect of pH on the Scn:$[Fe^{III}(Ent)]^{3-}$ system, and its relevance to normal cellular physiology, has not been studied previously.[17] Here we report comprehensive binding studies with Ent and wild-type recombinant Scn, as well as two Scn mutants incorporating mutations in the calyx designed to explore possible effects on pH-mediated ligand transitions. Fluorescence and UV-Vis spectroscopies have been used to determine Scn/siderophore dissociation constants and to characterize the coordination of iron over a wide pH range, in the presence of the wild-type and mutant proteins. In addition, X-ray crystallographic and extended X-ray absorption fine structure data have provided structural characterization of the protein/siderophore interactions. By probing the role of selected amino acids in

the binding pocket of the protein and investigating the effect of Scn binding on the coordination of ferric Ent upon acidification these studies provide mechanistic detail to Scn-mediated siderophore interception and intracellular iron delivery.

Results

Scn is stable at low pH. It has been previously reported that physiological iron release from Scn occurs in acidic intracellular compartments.[11,12,14,18,19] In the absence of an identified mammalian siderophore, we investigated the solution behavior of the Scn:$[Fe^{III}(Ent)]^{3-}$ complex to characterize possible iron-release mechanisms triggered by acidification. Most of the experiments were carried out in aqueous solutions buffered with various salts (1 mM sodium phosphate, formate or acetate) covering a wide pH range (from 1.5 to 8). Size exclusion chromatography confirmed the stability and monodispersivity of Scn in these buffers (data not shown); far-UV circular dichroism (CD) spectra of Scn (Fig. S2) over a pH range of 7.4 to 2.0 all exhibit a minimum at 216 nm, characteristic of β-sheet structure, indicating no significant change in secondary structure. The near-UV CD spectra (Fig. 2) provide information about overall aromatic side chain conformation. Unlike a related protein, tear lipocalin,[20] no decrease in intensity of the CD signal from pH 7.4 to 2.0 is observed for Scn. Thus, the Scn structure is stable over this wide pH range, consistent with the near-identical crystal structures of Scn determined at neutral (pH = 7.0) and acidic (pH = 4.5) conditions.[6,21]

Interactions between Scn and obligate salicylate Ent analogs. Previous studies have characterized a structural change in $[Fe^{III}(Ent)]^{3-}$, from catecholate to salicylate geometry around the metal ion, as pH falls (Fig. 2), with protonation occurring preferentially at the *meta*-hydroxyl oxygen of the catechols and iron coordination shifting to the *ortho*-hydroxyl oxygen and the amide oxygen.[22] However, the low-pH, salicylate form $[Fe^{III}(EntH_3)]^0$ is predicted to be sterically incompatible with binding in the Scn calyx, based on docking modeling, due to clashes with the walls of the inflexible calyx as the catechol rings move outward during the transition (Fig. S3). To confirm that salicylate-type iron coordination is incompatible with Scn binding, co-crystallization and binding assays were carried out with the synthetic analogs $[Fe^{III}(SERSAM)]^0$ and $[Fe^{III}(SER(3M)SAM)]^0$, which have been previously used as models of the protonated, salicylate-form of ferric-Ent (Fig. 3).[23] Such ferric complexes are strongly colored in solution, as a result of intense ligand-to-metal-charge-transfer (LMCT) transitions.[6,23,24] However, Scn crystals grown in the presence of the salicylate compounds are colorless (Fig. S4), as opposed to $[Fe^{III}(Ent)]^{3-}$ co-crystals, which are a deep wine-red in color, indicating that the protein does not bind ferric-salicylate complexes, even at the millimolar concentrations present in the crystallization trials.[6,24]

The equilibrium dissociation constant of Scn for a siderophore or metal-siderophore complex has previously been measured by fluorescence quenching.[6,25] In this procedure, aliquots of freshly prepared solutions of the ligand (6 μM) are added successively to a Scn solution (100 nM) and the fluorescence intensity of the mixture (λ_{exc} = 281 nm, λ_{em} = 340 nm) is measured after five minutes of equilibration. Fluorescence titrations were performed on $[Fe^{III}(SERSAM)]^0$ and $[Fe^{III}(SER(3M)SAM)]^0$, at pH 5.5 in order to ensure stability of the chelates in solution.[23] The fluorescence of Scn was not affected by the presence of the ferric salicylate complexes (Fig. 3). Fluorescence titrations were also performed on the ligands SERSAM and SER(3M)SAM at pH 7.4 (Fig. 3), showing that SERSAM specifically binds to Scn, but with a much weaker equilibrium dissociation constant (0.13 ± 0.02 μM) than apo-Ent, though the details of this interaction are unknown in the absence of a complex crystal structure. In contrast, SER(3M)SAM does not affect the protein fluorescence significantly, suggesting that SER(3M)SAM does not bind specifically to Scn even in the absence of bound iron, consistent with the presence of methyl substituents on SER(3M)SAM that increase steric clashes with Scn.

Design of mutations to probe the effect of Scn on pH-dependent ligand changes. The previous experiments confirm that binding to Scn sterically hinders catecholate to salicylate transformation; although it is possible that protein/ligand interactions may locally buffer the effects of pH changes in bulk solvent. Either effect may result in apparent pK_a shifts for the observed siderophore transitions in the presence of protein. Alternately, the low-pH induced transitions may drive release of ligand from Scn. To examine the degree that Scn constrains these processes, two mutant forms of Scn were

engineered: W79A/R81A, designed to open the calyx and more readily allow catecholate-to-salicylate transitions without impeding binding; and Y106F, designed to eliminate the sole hydrogen bond between Scn and the Ent catechol groups. The side-chains of W79 and R81 contribute to directly blocking ring movements associated with the transition,[6,26] while the hydroxyl of Y106 may affect the salicylate shift through hydrogen bonding to Ent *meta*-hydroxyl oxygens. Both Scn-Y106F and Scn-W79A/R81A were expressed and purified using protocols identical to those for the wild-type protein.[21] To analyze the effects of these mutations on ligand binding, fluorescence quenching assays were performed to quantitate the interactions between wild-type Scn, Scn-Y106F and Scn-W79A/R81A and the apo or ferric forms of Ent (Fig. 4 and Table 1). Both the Y106F and W79A/R81A mutations clearly affect the affinity for $[Fe^{III}(Ent)]^{3-}$: at pH = 7.4, W79A/R81A decreases the affinity by approximately 180-fold and Y106F by 50-fold, though both mutants retain specific recognition of $[Fe^{III}(Ent)]^{3-}$, with clear transitions apparent in the titrations and K_d values lower than 100 nM. The effects of the mutations are less pronounced on apo-Ent binding, with less than three-fold reductions in affinity observed at pH = 7.4. However, neither mutant binds the salicylate $[Fe^{III}(SERSAM)]^0$ and $[Fe^{III}(SER(3M)SAM)]^0$ complexes (Fig. 3), suggesting that, while calyx constraints on the salicylate coordination shift may be relaxed in the mutants, they have not been eliminated.

The W79A/R81A double mutation widens the Scn calyx. The crystallographic analysis of $[Fe^{III}(Ent)]^{3-}$ bound to the Scn-W79A/R81A mutant (Table S1) shows that these two substitutions do not affect the backbone conformation of Scn locally or globally (superposition rmsds of Scn-W79A/R81A onto wild-type Scn (PDB accession code 1L6M): 0.223 Å molecule A, 0.517 Å molecule B and 0.255 Å molecule C; calculated on all common Cα). No significant side-chain differences are apparent between the Scn-W79A/R81A mutant protein and previous wild type Scn structures except for the mutated residues. Therefore this double mutant achieves the goal of widening the Scn calyx, merging two pockets into one larger feature in the calyx (Fig. 5). While these mutations do not affect the structure of the protein, the enlarged calyx now affects how $[Fe^{III}(Ent)]^{3-}$ is bound. As in previous Scn:$[Fe^{III}(Ent)]^{3-}$ complex structures, the siderophore Ent is broken down during crystallization into a combination of monomeric units. However, while the wild type structure includes two 2,3-dihydroxybenzoic acid (2,3-DHBA) moieties in the pockets adjacent to W79 and R81 and a 2,3-dihydroxybenzoyl-serine (2,3-DHBS) molecule in the pocket delimited by K125 and K134, with enlargement of the calyx, there is now sufficient room for a 2,3-DHBS derivative to border on K125 and bind in an inverted orientation with the serine moiety pointing down towards the core of the protein (this has not been observed in any previous Scn structures). Additional contacts are made between the protein and the serine moiety in this pocket, including hydrogen bond interactions with S68 and Y106. Also, the increased calyx volume allows the 2,3-DHBA/2,3-DHBS catechol rings to redistribute around the iron center, causing the 2,3-DHBS placed between K125 and A81 to drop around 1 Å further into the pocket and the 2,3-DHBA unit adjacent to K134 to move up approximately 1 Å. Additionally, the plane of the phenyl ring between K125 and A81 rotates by approximately 30° in comparison to the wild type structure. Enlarging the calyx through this mutation would be predicted to more readily allow $[Fe^{III}(Ent)]^{3-}$ to undergo catecholate-to-salicylate transformations in response to acidification, though this mutation does not widen the calyx sufficiently to allow fully tri-salicylate ferric Ent, shown by the lack of binding of ferric SERSAM and SER(3M)SAM (see above). The W79A mutation eliminates some π-stacking interactions with Ent, and R81A eliminates potential cation-π interactions, but this mutant Scn still retains the cation-π interactions with the two remaining, positively-charged side-chains in the binding calyx (K125 and K134), considerable van der Waals contacts with the remaining catechol pocket in the calyx and the Y106 hydrogen bond.[6] These changes are therefore consistent with the 180-fold reduction in affinity observed for Ent binding.

Mutation of Y106 affects $[Fe^{III}(Ent)]^{3-}$ stability. The consequences of mutating Y106 to phenylalanine are more complicated than would be predicted from the simple loss of a single hydrogen bond partner. Crystallographic analysis of the structure of this mutant (Table S1 and Fig. 5) again shows no overall change in the structure of the protein (superposition rmsds of Scn-Y106F onto wild-type Scn (PDB accession code 1L6M): 0.221 Å molecule A, 0.305 Å molecule B and 0.232 Å molecule C; calculated on all common Cα) and essentially no local perturbation of the structure of the calyx, as

would be predicted with such a conservative substitution. However, it was observed that co-crystals of this mutant with $[Fe^{III}(Ent)]^{3-}$ were much paler in color than typical complexes, even with high molar ratios of ligand:protein (Fig. 5). The structure revealed the absence of bound iron and only a single serine-catechol fragment, likely 2,3-DHBS, bound in the pocket delimited by K125 and K134. This observation is likely explained by enhanced breakdown of $[Fe^{III}(Ent)]^{3-}$ in complexes with the Y106F mutant versus wild-type Scn in crystallization buffer (pH = 4.5) over the course of crystallization (more than two weeks). The effect is likely not rapid enough to affect the fluorescence quenching binding assay. However, this mutation also achieves the intended goal of eliminating a hydrogen bond that may affect pH-induced ligand transitions without otherwise altering the conformation of other calyx components, though, again, not sufficiently to allow the obligate salicylate compounds SERSAM and SER(3M)SAM to bind, ± iron (see above). The 50-fold reduction in affinity associated with this mutation is also consistent with the loss of a single, strong hydrogen bond. It is noteworthy that the only pocket in the Scn calyx to retain a catechol moiety is that adjacent to K125 and K134, suggesting that this pocket has the highest affinity for a catechol group among the three pockets in the calyx and may be the most important for defining specificity.

pH dependence of Scn/Ent interactions: fluorescence spectroscopy. Having confirmed that the Scn mutations had the desired effects, fluorescence quenching binding assays were performed with wild-type Scn, Scn-W79A/R81A and Scn-Y106F, at selected pH values, on Ent and its ferric complex, to examine the influence of pH on protein binding (Fig. 6 and S5). The pH values (7.4, 5.5, 4.0, 3.0 and 2.0) were chosen to bracket the three pK_a values of $[Fe^{III}(Ent)]^{3-}$ (pK_{a1} = 5.2, pK_{a2} = 3.2, pK_{a3} = 2.7), which correspond to the stepwise protonation of the *meta*-hydroxyl oxygens of the catecholate rings in aqueous solution (Table 1).[24] The individual affinities of each form of Scn for $[Fe^{III}(Ent)]^{3-}$ are essentially constant down to pH 4.0, followed by a drastic, almost 300-fold increase in K_d between pH 4.0 and 3.0, a pH range corresponding to the second protonation step of $[Fe^{III}(Ent)]^{3-}$ in solution. The presumption is that binding becomes weaker as $[Fe^{III}(Ent)]^{3-}$ becomes protonated, as it transforms to salicylate coordination. These titrations also show complete loss of siderophore binding below pH = 3.0 for wild-type and mutant Scn. Neither Scn mutation permits binding at lower pH than wild-type and, indeed, both show loss of binding at higher pH values than wild-type (< 4.0).

Another pair of experiments monitored the fluorescence of preformed Scn:$[Fe^{III}(Ent)]^{3-}$ and Scn:Ent complexes upon acidification. The fluorescence of the protein was quenched as the ligand was added at pH 7.4, reaching a plateau at a protein:ligand stoichiometry of 1:1. Hydrochloric acid was then added to the solution, with reductions in fluorescence quenching beginning near pH 3.5. Below this pH the protein fluorescence increased back to its original, unquenched value at a pH around 2 (Fig. 7 and S6). These data show that Scn starts releasing its ligand below pH 3.5, with maximal release at pH $\leq$ 2. While similar experiments described in previous reports[12,18] used ^{59}Fe as a tracer, use of fluorescence spectroscopy here allowed measurement of apo-siderophore titrations as well, indicating that both apo- and ferric-Ent exhibit the comparable behavior and are fully released from Scn at sufficiently low pH.

pH dependence of Scn/Ent interactions: UV-Vis spectroscopy. Data reported in a previous study showed that iron-loaded Scn releases labeled ^{59}Fe in acidic conditions.[12] However, iron may be released as free ferric ion, $[Fe^{III}(Ent)]^{3-}$ or an intermediate species potentially available for uptake by other receptors. To examine the coordination features of the ferric complex upon release from the protein, spectrophotometric thermodynamic measurements were performed on complexes of $[Fe^{III}(Ent)]^{3-}$ with the wild-type Scn, Scn-W79A/R81A and Scn-Y106F. The three pK_a values of $[Fe^{III}(Ent)]^{3-}$ corresponding to the stepwise protonation of the phenolate oxygens can be determined by spectrophotometric titrations. Refinement of the absorbance data was performed by exploiting the intense broad LMCT band of the ferric complex. The salicylate shift of $[Fe^{III}(ent)]^{3-}$ at very acidic pH can be followed by the shift in energy of the intense $\pi \rightarrow \pi^*$ transition around 300 nm.[22,24] Different protein:$[Fe^{III}(ent)]^{3-}$ complexes were titrated (Fig. 8 and S7) to the free ferric complex in aqueous solution, over a wide pH-range. The salicylate coordination shift is not observed with protein-siderophore complexes. For all three Scn:$[Fe^{III}(Ent)]^{3-}$ complexes, the characteristic LMCT and $\pi \rightarrow \pi^*$ transition bands of $[Fe^{III}(Ent)]^{3-}$ first increase, with a slight shift to higher energies for the latter, and then decrease to finally vanish at low pH, indicated by a shoulder remaining at λ = 318 nm.

Nevertheless, factor analysis of the titration curves in all cases showed three sequential protonation equilibria corresponding to log K_a values reported in Table 2; the best nonlinear least-squares refinements were obtained with the models including four species that absorb significantly. While the shift to more intense and energetic $\pi \rightarrow \pi^*$ transitions is characteristic of hydrolysis of the tri-serine lactone in the complex,[27] the disappearance of both absorption bands indicate a loss of coordination at the metal center.[24] These results show that wild-type Scn and the two Scn mutants do not affect the third protonation event (pK_{a3}), as neither apo nor ferric Ent bind at this pH, but that protonation events at pH values between neutrality and 3.0 likely favor hydrolysis of the three ester bonds in the Ent backbone rather than protonation of the phenolate oxygens. This is consistent with binding in the Scn calyx acting to buffer Ent catechol protonation, either by steric effects preventing salicylate transitions or by interactions with protein groups directly shifting the pK_a's of these oxygens. Protonation of the Ent backbone would then be consistent with driving degradation, with the effect most pronounced with the two Scn mutants.

pH dependence of Scn/Ent interactions: EXAFS spectroscopy. Fe K-edge EXAFS measurements have previously been used to follow $[Fe^{III}(Ent)]^{3-}$ catecholate-to-salicylate coordination shifts upon acidification and protonation. Here we compare the pH-dependent solution behaviors of free and Scn-bound $[Fe^{III}(Ent)]^{3-}$ (Table 3).[23] Though good quality data extended to at least k = 12.0 $Å^{-1}$ in most cases, a limited k range was analyzed by Fourier transformation (2.5 – 10.5 $Å^{-1}$) to remain consistent with previous studies.[23] Due to the short k range employed, the analysis focused on fitting only the first oxygen shell with fewer degrees of freedom. Sequestration of $[Fe^{III}(Ent)]^{3-}$ by Scn at pH 7.4 did not affect the first coordination sphere of the ferric complex (Fig. S8). Moreover, independent fits of the free and protein-bound ferric complex EXAFS spectra show identical Fe-O distances for both *ortho* and *meta* oxygen atoms of the catecholate rings. The average Fe-O distance is the same as in the solid form of $[Fe^{III}(Ent)]^{3-}$ within experimental error.[23] Upon acidification to pH values lower than 3.5, a drop in the Fourier transform magnitude, as well as line shape changes occur (Fig. 9). In addition, the fit for the Scn-bound ferric complex at pH 2.5 (Fig. S8) shows longer average Fe-O distances than at pH 7.4 and the disorder (as indicated by the Debye-Waller factor, σ^2) between *ortho* and *meta* oxygens is significantly larger. This result is inconsistent with a salicylate coordination transformation, in which case the average Fe-O distance would be shortened. Furthermore, comparisons between the X-ray diffraction structures of the hexadentate $[V^{IV}(Ent)]^{2-}$ and tris-bidentate $[V^{IV}(eba)_3]^{2-}$ complexes (where eba is the bidentate *N*-2,3-dihydroxybenzoyl-ethyl moiety) have shown that the disorder in V-O distances is greater in the case of the ethyl-substituted catecholamide species, which is not constrained by a rigid scaffold.[28] A tris-bidentate ferric complex of the hydrolyzed monomer 2,3-DHBS, $[Fe^{III}(2,3\text{-}DHBS)_3]^{3-}$, would also show a higher disorder in Fe-O distances than the parent complex $[Fe^{III}(Ent)]^{3-}$ incorporating the rigid tri-serine lactone. Binding to Scn therefore favors cleavage of the Ent backbone and formation of a tris-catecholate ferric complex with three 2,3-DHBS groups, instead of a salicylate coordination shift, upon acidification.

HPLC analysis of pH-induced Scn release products. To determine whether Ent is still intact after release from Scn at low pH, solutions of apo-Scn, Scn bound to $[Fe^{III}(Ent)]^{3-}$ and $[Fe^{III}(Ent)]^{3-}$ were prepared at pH 7.4 and then acidified to pH 2.5. Released ligands were separated from protein by ultrafiltration and purified by HPLC to further separate iron from Ent or Ent breakdown products. At pH 7.4, the complex $[Fe^{III}(Ent)]^{3-}$ remains bound to the protein and no siderophore derivative is present in the filtrate. Acidification of Scn:$[Fe^{III}(Ent)]^{3-}$ essentially releases only the monomer 2,3-DHBS (identified by mass spectrometry, retention time: 4.9 min) and no intact Ent, as opposed to acidification of $[Fe^{III}(Ent)]^{3-}$ that results in deferration from the unbroken siderophore (Fig. 10).

Discussion

Two distinct roles have previously been attributed to Scn.[16] First, Scn functions as an anti-microbial component of innate immunity, scavenging, sequestering and depleting bacterial ferric- and apo-siderophores.[5,7] Second, Scn functionally acts as a growth factor in multiple cell types, able to modulate various cellular responses, including proliferation, apoptosis, and differentiation.[16] It has been reported that some of these cellular responses are markedly affected by the ligand state of Scn (whether the protein is carrying a ferric siderophore or not), though most of these experiments have depended upon using Ent as a surrogate in the absence of a characterized endogenous siderophore.[12,14,18] It is possible that Ent itself serves this function in normal physiology, though, in the absence of an active infection, the only source of Ent would be the normal colonizing microbiota of the gastrointestinal tract and there is no evidence that siderophores are secreted routinely, or are capable of being absorbed, from this source. It seems more likely that some alternate compound serves as the endogenous siderophore mediating Scn physiological iron transport, either synthesized endogenously or from some environmental source, and there are several reports providing indirect evidence for the existence of such a compound.[12,18] However, the structural studies strongly argue that such a compound would likely be closely related to Ent, justifying its use here and in previous studies as a surrogate.

Upon acidification, protonation of $[Fe^{III}(Ent)]^{3-}$ free in solution occurs in three discrete one-proton steps at the *meta*-hydroxyl oxygens of the catechols, resulting eventually in the triprotonated, salicylate, neutral complex $[Fe^{III}(EntH_3)]^0$. Coordination of the *ortho*-hydroxyl oxygens causes the catechols to rotate around the amide bond (Fig. 2), thereby increasing the effective width of the ligand. This structural change in the siderophore, modeled by the synthetic analogs SERSAM and SER(3M)SAM, impedes binding of the ferric complexes thereof to Scn. This result could be explained by either of two separate mechanisms: steric constraints imposed by the relatively rigid protein calyx or loss of a complementary electrostatic charge, as the obligate salicylate compounds, SERSAM and SER(3M)SAM, form neutral complexes with iron. However, two lines of evidence show that the failure of ferric SERSAM and SER(3M)SAM to bind Scn is likely primarily due to steric considerations alone and not loss of electrostatic interactions with the protein, though electrostatics almost certainly contributes significantly to overall affinity. Firstly, we show that apo-Ent, a weakly-charged species, binds strongly to Scn, displaying nanomolar dissociation constants at pH values down to 4.0 (Table 1). Secondly, Y106F also fortuitously demonstrates that neutrally-charged species can still bind to Scn through other interactions in the calyx, shown by the retention of an uncharged serine-dihydroxy benzoate between K125 and K134.

While the conformation of Scn in solution remains stable over a wide pH range, as confirmed here by CD, the binding properties of the protein are markedly altered in very acidic solutions. Fluorescence quenching measurements show a slight decrease in the affinity of the recombinant wild-type and mutant proteins for both ferric- and apo- forms of Ent in mild acidic conditions while further acidification (pH < 4) weakens affinity substantially. Although the charge of the apo-ligand is not as drastically affected by acidification (the ligand is only partially deprotonated at pH 7.4),[24] protonation induces a conformational change, with rotation of 180° about the catechol-carbonyl bond, which modifies significantly the spatial occupancy of the ligand in solution (Fig. 2).

Previous studies using fluorescently labeled Scn and radiolabeled ^{59}Fe have shown that low pH drives release of iron from the protein into vesicles.[12,16,18,19] However, little emphasis was placed on the nature of the released iron or the release mechanism itself. Therefore, in addition to the binding specificity of Scn, the properties of the adducts formed by the protein with $[Fe^{III}(Ent)]^{3-}$ and Ent, respectively, were examined as functions of the acidity of the protein environment. The intrinsic fluorescence of Scn was monitored upon ligand addition followed by acidification, revealing that, for both $[Fe^{III}(Ent)]^{3-}$ and Ent, the ligand is released as the pH is decreased below 4. Furthermore, spectrophotometric acid titrations were performed on the adducts protein:$[Fe^{III}(Ent)]^{3-}$ formed with Scn, Scn-W79A/R81A and Scn-Y106F. Analysis of the absorption spectra showed no evidence of a salicylate coordination shift undergone by the ferric complex upon ligand release by the protein, but the $\pi \rightarrow \pi^*$ transition shifted to higher energy levels and the ligand-to-metal-charge-transfer band characteristic of the ferric complex disappeared progressively in all complexes, indicative of scaffold hydrolysis and release of free iron

from the ferric complex. The EXAFS spectra and corresponding Fourier transform data collected from the neutral and low pH solutions of Scn:$[Fe^{III}(Ent)]^{3-}$ are also inconsistent with formation of a salicylate-bound complex. Analysis of the EXAFS data and comparison to previously described structures of $[V^{IV}(Ent)]^{2-}$ complex derivatives indicates a loss of coordination around the metal center upon acidification and suggests the presence, at low pH, of a degraded intermediate complex in which the enterobactin trilactone is cleaved. The absence of intact ligand in Scn structures determined from crystals grown in acidic conditions (pH = 4.5), where breakdown preferentially occurred in the triserine backbone, complements the behavior in solution. Degradation of Ent to the bidentate monomer 2,3-DHBS was confirmed by analysis of acidic filtrates collected after centrifugation and filtration of the low pH protein adduct solution.

Common iron-related strategies developed by the mammalian host focus on limiting the available extracellular iron to prevent bacterial proliferation; expression of iron-binding proteins such as transferrin, lactoferrin and ferritin and production of hepcidin are enhanced during infection, resulting in the reduction of serum iron levels and uptake of iron by enterocytes, hepatocytes or macrophages.[3,29,30] It would therefore be plausible that Scn intervenes to retrieve host iron from the ferric-siderophore complex and to convey the metal to intracellular spaces. Similar to transferrin, the release of iron from Scn depends on the passage of the protein through acidic late endosomes.[12] The data presented here show that acidification of Scn bound to $[Fe^{III}(Ent)]^{3-}$ triggers the release of both iron and degraded Ent only at very low pH (pH < 3) *in vitro*. However, the minimum pH in late endosomes (~ 5.0) is not low enough to remove iron from the Scn:$[Fe^{III}(Ent)]^{3-}$ complex effectively, yet cells are capable of doing so with notable efficiency. This conundrum can be resolved in several ways. In one scenario, Ent does not serve as the endogenous siderophore mediating physiological iron transport, but rather a compound, as yet unidentified, that releases iron from Scn complexes at more moderate pHs. While having the advantage of not depending upon bacterial synthesis for an important component of iron transport, this scenario implies that iron sequestered as Scn/bacterial siderophore complexes is simply lost from the body.

However, our results show that, at endosomal pH, the Scn:$[Fe^{III}(Ent)]^{3-}$ complex undergoes hydrolysis of the tri-serine lactone backbone, resulting in the formation of a tris-bidentate complex $[Fe^{III}(2,3\text{-}DHBS)_3]^{3-}$ which remains bound to Scn. Cleavage of the Ent backbone does not affect the stabilizing electrostatic/cation-π interactions in the complex, and therefore does not result in release of ligand on its own. On the other hand, the reduction potential of the ferric complex (-750 mV *vs* NHE for $[Fe^{III}(Ent)]^{3-}$) does increase considerably with backbone hydrolysis (-350 mV *vs* NHE for $[Fe^{III}(2,3\text{-}DHBS)_3]^{3-}$), within range of physiological reductants[31] such as ferrireductases, which have been observed in late endosomes.[32] In the alternate mechanism that resolves the conundrum, reduction of the metal center would then result in dissociation of ferrous iron from Scn-siderophore complexes. Scn has also been co-localized with the divalent metal transporter DMT1[12] (also called Nramp2 and DCT1) which is found in late endosomes[33] and is a good candidate for active transport of released ferrous iron.[34] In addition, the cell surface receptors for Scn[14,35] may play a role not only in binding Scn but also in promoting iron release from the protein at endosomal pH, as is seen in the case of transferrin.[34]

Thus the pH-dependency of the Scn/Ent interaction is consistent with siderophore hydrolysis and consequent release of ferrous iron in acidic intracellular compartments. While mild acidification of Scn:$[Fe^{III}(Ent)]^{3-}$ alone is not sufficient for iron release, it provides access to a pathway by which host iron may be recovered from bacterial iron scavengers.

Conclusion

Despite its high efficiency at chelating iron, the siderophore Ent is insufficient for establishing virulence of invading pathogens, since its ferric complex is sequestered by the innate immune system protein Scn. However, increasing data show that Scn also functions as an endogenous iron transporter independent of transferrin-mediated pathways. Since iron release has been shown to occur from Scn in low pH endosomes, protein mutagenesis, X-ray diffraction, as well as fluorescence, UV-visible and EXAFS spectroscopies were used to probe the pH dependence of siderophore recognition by Scn. The catecholate ferric Ent complex is stabilized when bound in the Scn calyx. However, the binding of Ent and its ferric complex by wild-type or mutant Scn is altered upon acidification or coordination change. Furthermore, hydrolysis of the tri-serine lactone of enterobactin is favored in the Scn:$[Fe^{III}(Ent)]^{3-}$ complex at mildly acidic pH, leading to the formation of Scn:$[Fe^{III}(2,3\text{-}DHBS)_3]^{3-}$. In this form, the ferric ion is more susceptible to physiological reduction and subsequent release, which could play a role in intracellular iron delivery.

Experimental Section

General. The ligands enterobactin, SERSAM and SER(3M)SAM as well as the ferric complexes $[Fe^{III}(Ent)]^{3-}$, $[Fe^{III}(SERSAM)]^{0}$ and $[Fe^{III}(SER(3M)SAM)]^{0}$ used for binding experiments with siderocalins were prepared as described previously.[23] All chemicals were obtained from commercial suppliers and were used as received. Corning high performance combination glass electrodes (response to $[H^+]$ was calibrated before each titration)[36] were used together with either an Accumet pH meter or a Metrohm Titrino to measure the pH of the experimental solutions. All aqueous solutions were prepared using distilled water that was further purified by passing through a Millipore Milli-Q reverse osmosis cartridge system.

Protein Expression. The Scn-W79A/R81A and Scn-Y106F mutants were made by site-directed mutagenesis of the pGex-4T3 C87S construct of human Siderocalin using the following primers: 5'-GAAGTGTGACTACGCGATCGCGACTTTTGTTCCAGGTTCCCAGCCCGGCG-3' (forward) and 5'-CGCCGGGCTGGGAACCTGGAACAAAAGTCGCGATCGCGTAGTCACACTTC-3' (reverse) for Scn-W79A/R81A; 5'-GATTAACGAGTTTCCTCGTCCGAGTG-3' (forward) and 5'-CAGTCGGACGAGGAAACTCGTTAATC-3' (reverse) for Scn-Y106F. Protein purification was then performed as previously described.[37] The DNA was transformed into the *E. coli* strain BL21-DE3-Codon Plus-RIL by electroporation. Bacteria were grown in LB medium containing ampicillin and chloramphenicol until early-log stage, were induced with 1mM IPTG and incubated for 4 hours at 37 °C. The bacteria were pelleted by centrifugation and washed with PBS buffer at pH 7.4. Pellets were resuspended in PBS buffer (pH 7.4) with 1 mM PMSF and sonicated, and cell debris was removed by centrifugation. The supernatant containing the fusion protein was loaded onto a glutathione Sepharose column, and the recombinant protein was obtained after cleavage of the GST tagged protein by incubation off the column for one hour with thrombin in PBS buffer (1.37 M, 27 mM KCl, 100 mM Na_2HPO_4, 20 mM KH_2PO_4, pH 7.4). The eluted protein was finally purified by size exclusion chromatography, performed using a Superdex p75 column (GE Healthcare Life Sciences) in PNEA (25mM PIPES, 150mM NaCl, 1mM EDTA and 0.02% NaN_3, pH 7.0). Scn was stored at mM concentrations in PBS aqueous buffer (pH 7.4) at 4 °C. The concentration of various protein solutions (recombinant wild type and mutants) was first estimated using a standard bicinchoninic acid (BCA) protein assay. More accurate concentration determination was achieved by UV-Vis spectroscopy, using a published extinction coefficient value (λ = 29930 M^{-1} cm^{-1} at λ = 280 nm).[38] UV-Visible absorption spectra were taken on a Varian Cary 300 UV-Vis spectrometer.

CD Spectroscopy. Protein samples were prepared in phosphate/formate/acetate buffered aqueous solutions (1 mM) to control the pH from 2.0 to 7.4. CD spectra were recorded on a Jasco J-810 spectropolarimeter with cuvettes of 1 and 10 mm path length containing 5 and 60 μM protein for far- and near-UV spectra, respectively.

Fluorescence Quenching Binding Assay. Fluorescence quenching of recombinant wild-type and mutant Scn was measured on a Jobin Yvon fluoroLOG-3 fluorometer with 3 nm slit band pass, using the characteristic excitation and emission wavelengths λ_{exc} = 281 nm and λ_{em} = 340 nm. The intrinsic fluorescence in proteins is generally attributed to tryptophan residues; two residues W31 and W79 are found in the proximity of the Scn binding site. Measurements were made at a protein concentration of 100 nM in buffered aqueous solutions, 5% DMSO, plus 32 μg/mL ubiquitin. Fluorescence values were corrected for dilution upon addition of ligand. Fluorescence data were analyzed by nonlinear regression analysis of fluorescence response versus ligand concentration using a one-site binding model as implemented in DYNAFIT.[39] The K_d values are the results of at least two independent titrations. All standard binding experiments were done at pH 7.4 using Tris-buffered saline (TBS). The pH-dependent experiments were carried out in an aqueous mixture of phosphate, formate, and acetate sodium salts (5 mM) to allow pH variations from 1.5 to 8. Titrations of salicylate complexes were performed at pH 5.5. Control experiments were done with ferric enterobactin at pH 7.4 to ensure that different buffering salts and DMSO would not impair the measurements, as well as with the free protein at different pH values.

Ligand Solutions Preparation. Ligand solutions were freshly prepared *in situ*. An aliquot of a DMSO stock solution of the free ligand (4 mM, 25 μL) and $FeCl_3$ salt (27 mM, 1 eq., solution standardized by EDTA titration according to the methods of Welcher[40]) were combined, vigorously

shaken and diluted with TBS buffer to form the tris-catecholate complexes at a concentration of 0.1 mM (no metal added for the titrations of apo-enterobactin). The solutions were equilibrated for 2h, diluted to a final concentration of 60 μM in 5% DMSO/aqueous buffer and adjusted to the desired pH. For the salicylate complexes, the same procedures were followed, but using DMSO stock solutions of $[Fe^{III}(SERSAM)]^0$ and $[Fe^{III}(SER(3M)SAM)]^0$ and diluting to pH 5.5 solutions.

Crystallography. The mutated proteins Scn-W79A/R81A and Scn-Y106F were isomorphously co-crystallized with ferric enterobactin using the same crystallization conditions as previously reported for the wild-type protein.[6,26] Co-crystals were grown by vapor diffusion at 22 °C over reservoirs of 1.4-1.8 M ammonium sulfate, 50-100 mM sodium chloride, buffered at pH 4.5 with 100 mM sodium acetate. Suitable crystals were cryprotected by supplementing mother liquor with 15% glycerol prior to flash-cooling at -170 °C. The diffraction data were collected with a Rigaku Raxis IV++ area detector using CuKα radiation and processed with the HKL2000 software package.[41,42] Reflections chosen for calculating R_{free} for both Scn-W79A/R81A and Scn-Y106F datasets were matched to those selected for the wild-type structure (PDB code 1L6M). Phases were calculated by using the wild type Scn structure. Modeling was performed with Coot[43] and the structures were refined using Refmac5.[44] Relevant data collection and refinement statistics are shown in Table S1. Coordinates for the structures have been deposited with the PDB (accession codes 3BYO and 3CBC for Scn-W79A/R81A and Scn-Y106F respectively).

Solution Thermodynamics. Titrations were performed and thermodynamic parameters were determined using procedures and equipment following previous descriptions.[45-47] Metrohm autoburets (Dosimat or Titrino) were used for incremental addition of acid or base standard solutions to the titration cell. The titration instruments were fully automated and controlled using LabView software.[48] Titrations were performed in 0.1 M KCl supporting electrolyte under positive Ar gas pressure. The temperature of the experimental solution was maintained at 25 °C by an external circulating water bath. UV-Visible spectra for incremental titrations were recorded on a Hewlett-Packard 8452a spectrophotometer (diode array). Solid reagents were weighed on a Metrohm analytical balance accurate to 0.01 mg. Titrants were degassed by boiling for 1 h while being purged under Ar. Carbonate-free 0.1 M KOH was prepared from Baker Dilut-It concentrate and was standardized by titrating against potassium hydrogen phthalate using phenolphthalein as an indicator. Solutions of 0.1 M HCl were similarly prepared and were standardized by titrating against sodium tetraborate to Methyl Red endpoint.

Protonation Constants: Spectrophotometric Titrations. The protonation constants of ferric enterobactin in the different protein environments were determined by spectrophotometric titration. Solutions were assembled from an aliquot of the Scn:$[Fe^{III}(Ent)]^{3-}$ adduct in PBS buffer at pH 7.4 and the supporting electrolyte solution, with resulting ligand concentrations between 50 and 100 μM. Constant buffering of the solution was assured by the addition of glycine, formate, acetate and Mes buffers (1 mM). An average of 20 data points were collected in each titration (adding acid), each data point consisting of a pH measurement and an absorbance spectrum over the pH range 7.4 to 1.8.

Data Treatment. All equilibrium constants were defined as cumulative formation constants, β_{0lh} according to equation 1, where the protein adduct is designated as L. Stepwise protonation constants, K_a^n, may be derived from these cumulative constants according to equation 2. For each protein mutant, two non-reversible titrations were conducted against HCl only and combined for simultaneous refinement. Only the proton concentration was allowed to vary in the spectrophotometric studies, and all other concentrations were held at estimated values determined from the volume of standardized stock and absorbance values of the protein:$[Fe^{III}(Ent)]^{3-}$ adducts at pH 7.4 measured after 12 hours equilibration. Nonlinear least squares refinement of the adducts proton association constants was accomplished using the program pHab.[49] The four species formed with the catecholamide subunits were considered to have significant absorbance to be observed in the UV-Vis spectra. Analysis was performed over the spectral range λ = 290-650 nm.

$$L + hH^+ \leftrightarrow H_hL \qquad \beta_{0lh} = \frac{[H_hL]}{[L][H^+]^h} \qquad (\mathbf{1})$$

$$K_a^n = \frac{[H_n L]}{[H_{n-1} L][H^+]} = \frac{\beta_{0ln}}{\beta_{0l(n-1)}} \qquad (2)$$

Extended X-ray Absorption Fine Structure Measurements. Solutions of Scn (4 mM) were incubated with an equimolar amount of ferric enterobactin (4 mM) in an aqueous buffer (0.25 M, pH 7.4) composed of glycine, sodium formate, bistrispropane and tricine to allow a wide range of pH without interfering with the EXAFS spectra. For all samples (pH 7.4 to 2.5), the pH was adjusted with concentrated nitric acid (70%), solutions were flushed with Argon, equilibrated, ultracentrifugated and treated with glycerol (10%). EXAFS measurements were performed on beamline 2-3 at the Stanford Synchrotron Radiation Laboratory (SSRL). A Si (220) double crystal monochromator was used to collect the iron K-edge (7112 eV) spectra, with an operating ring current of 100 mA. Fluorescence spectra were recorded at 15 K in an Oxford flow-through He cryostat with a Canberra Ge-13 element detector. Gas ionization chambers were filled with nitrogen gas and the x-ray beam was defined using 1×10 mm slits. The incident beam was detuned 50% to limit its harmonic content. Data were collected at the Fe K-edge to a value of k = 16 $Å^{-1}$. To ensure consistency with previous studies,[23] fits were transformed over the k-range 2.5-10.5 $Å^{-1}$, which limited the analysis to the first oxygen shell. Absorption spectra were fit and analyzed using the Artemis code.[50] The coordination number N was constrained to 6 and the amplitude reduction factor S_0^2 and energy origin E_0 were constrained according to fits of the structurally characterized model compound $[Fe^{III}(TRENCAM)]^{3-}$.[23] The fitting model included single-scattering shells from first-shell oxygens which were assumed to share the same Debye-Waller factor σ^2 and ΔR. Fourier transforms over a longer k-range (2.5-12.5 $Å^{-1}$) and analysis using alternative models that included additional degrees of freedom confirmed that only two variables were needed in this analysis.

Acidification and HPLC analysis. Scn samples (0.1 mM) were prepared at pH 7.4 in an aqueous mixture of phosphate, formate and acetate sodium salts (1 mM). Ferric-enterobactin (0.1 mM) was added to the protein and the solution was incubated overnight at 4 °C. The solution was then acidified to pH 2.5 and washed with 5 volumes of buffer (pH 2.5), before being brought back to pH 7.4. High Pressure Liquid Chromatography runs were performed at each stage of this procedure, by injection of 20 μL of filtered solutions (0.22 μm) through a reverse-phase analytical C-18 column. A gradient from 5% CH_3CN in ddH_2O/0.1%TFA to 50% CH_3CN in ddH_2O/0.1% TFA over 20 min at 1 mL/min was used to elute enterobactin and its derivatives (detection by UV-Vis absorption at 316 nm and identification by electrospray mass spectrometry). Controls followed the same experimental setup but without iron or siderophore added. The injection peak (R_t = 1.4 min) was not characterized but is most likely resulting from the high salt composition of the solutions. The sample filtrates are eluted in acidic conditions, therefore the solutions of $[Fe^{III}(Ent)]^{3-}$ at pH 7.4 and 2.5 both result in a peak corresponding to apo-Ent. Ent (M^+, m/z calc. 669.1, obs. 669.6, R_t = 16.3 min) and 2,3-DHBS (M^+, m/z calc. 241.1, obs. 240.1, R_t = 4.9 min) were detected with positive and negative ion modes, respectively.

Acknowledgment. This research was supported by the National Institutes of Health (K.N.R.: AI11744, R.K.S.: AI59432). The authors thank Trisha Hoette for many helpful discussions, Wendy Paulsene for help in creating the Siderocalin mutants, and the SSRL staff for their assistance. EXAFS measurements were carried out at the SSRL, a national user facility operated by Stanford University on behalf of the U.S. DOE, Office of Basic Energy Sciences. The SSRL Structural Molecular Biology Program is supported by the U.S. DOE, Office of Biological and Environmental Research, and by the National Institutes of Health, National Center for Research Resources, Biomedical Technology Program. D.K.S. and J.A.W. were supported by the Director, Office of Science, Office of Basic Energy Sciences, Division of Chemical Sciences, Geosciences, and Biosciences of the U.S. Department of Energy at LBNL under Contract No. DE-AC02-05CH11231.

Supporting Information Available: Full citation for reference 18; additional figures and spectral data obtained for the fluorescence and spectrophotometric titrations of the various mutants of Scn in the

presence of apo- and ferric- enterobactin; EXAFS Fourier transforms and table of crystallographic statistics. This material is available free of charge via the Internet at http://pubs.acs.org.

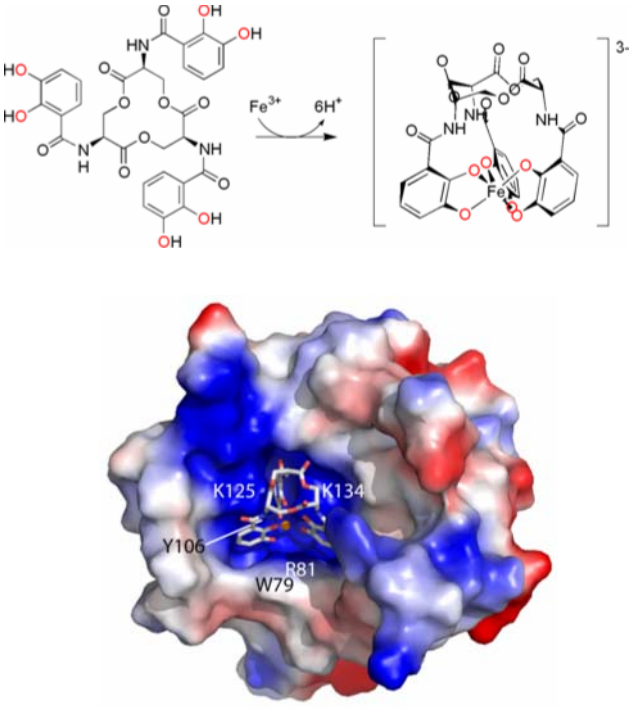

Figure 1. Complexation of ferric ion by the siderophore enterobactin (top, the iron coordinating atoms are indicated in red) and specific binding of the ferric complex of enterobactin $[Fe^{III}(Ent)]^{3-}$ by the mammalian protein Scn (bottom).

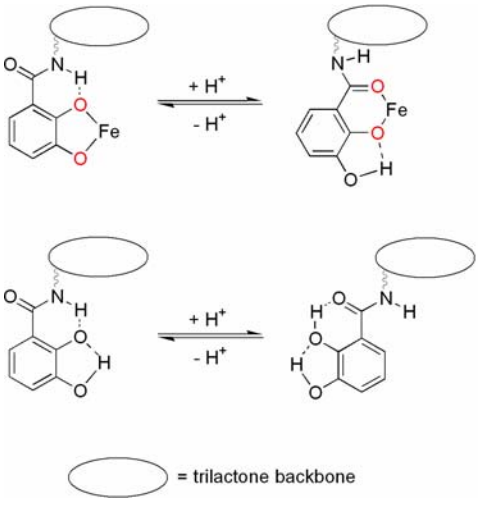

Figure 2. Conformation changes undergone by ferric- (top) and apo- (bottom) enterobactin upon protonation. The coordination of the iron center shifts from catecholate (top left) to salicylate (top right) as the complex is protonated, and the catecholate rings rotate around the amide bonds as the free ligand is protonated.

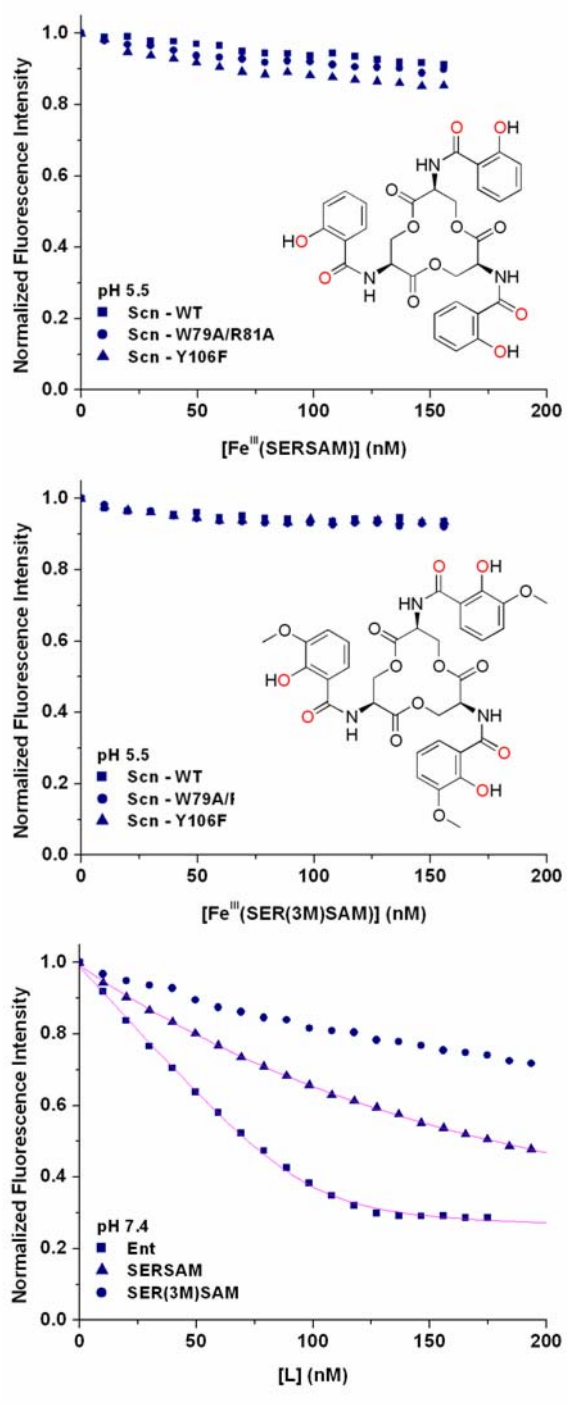

Figure 3. Fluorescence quenching analyses of the binding of the wild type Scn (Scn-WT) and the two mutants Scn-Y106F and Scn-W79A/R81A with the ferric complexes of the salicylate analogs of Ent: $[Fe^{III}(SERSAM)]^0$ (top) and $[Fe^{III}(SER(3M)SAM)]^0$ (middle), at pH 5.5 (the iron-coordinating oxygen atoms are indicated in red). Bottom: fluorescence quenching analyses of Scn-WT binding with the ligands SERSAM and (SER(3M)SAM) at pH 7.4. Symbols give the fluorescence data at 340 nm, and lines give the calculated fits to a one-binding site model.

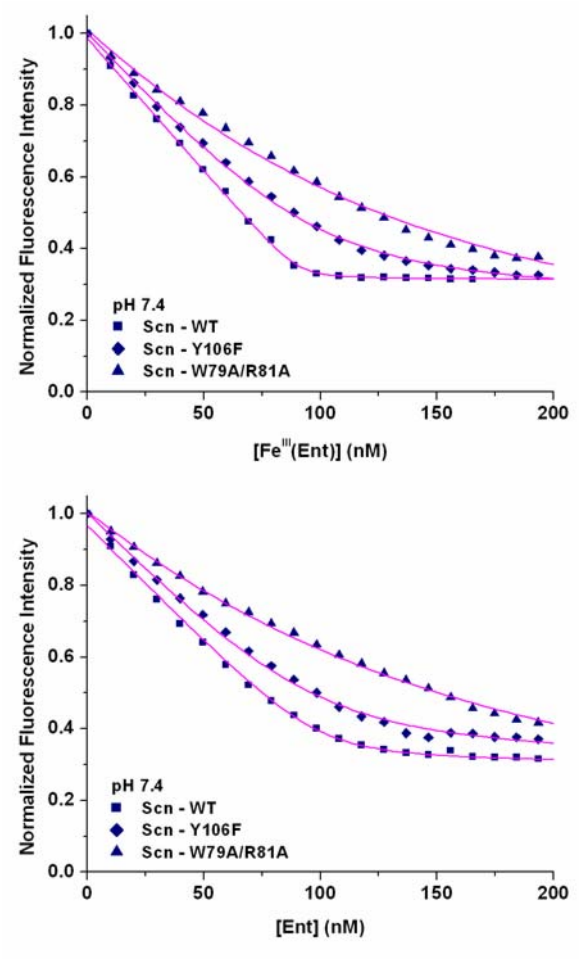

Figure 4. Fluorescence quenching analyses of the binding of the wild type Scn (Scn-WT) and the two mutants Scn-Y106F and Scn-W79A/R81A with ferric (top) and apo (bottom) enterobactin. Symbols give the fluorescence data at 340 nm, and lines give the calculated fits to a one-binding site model.

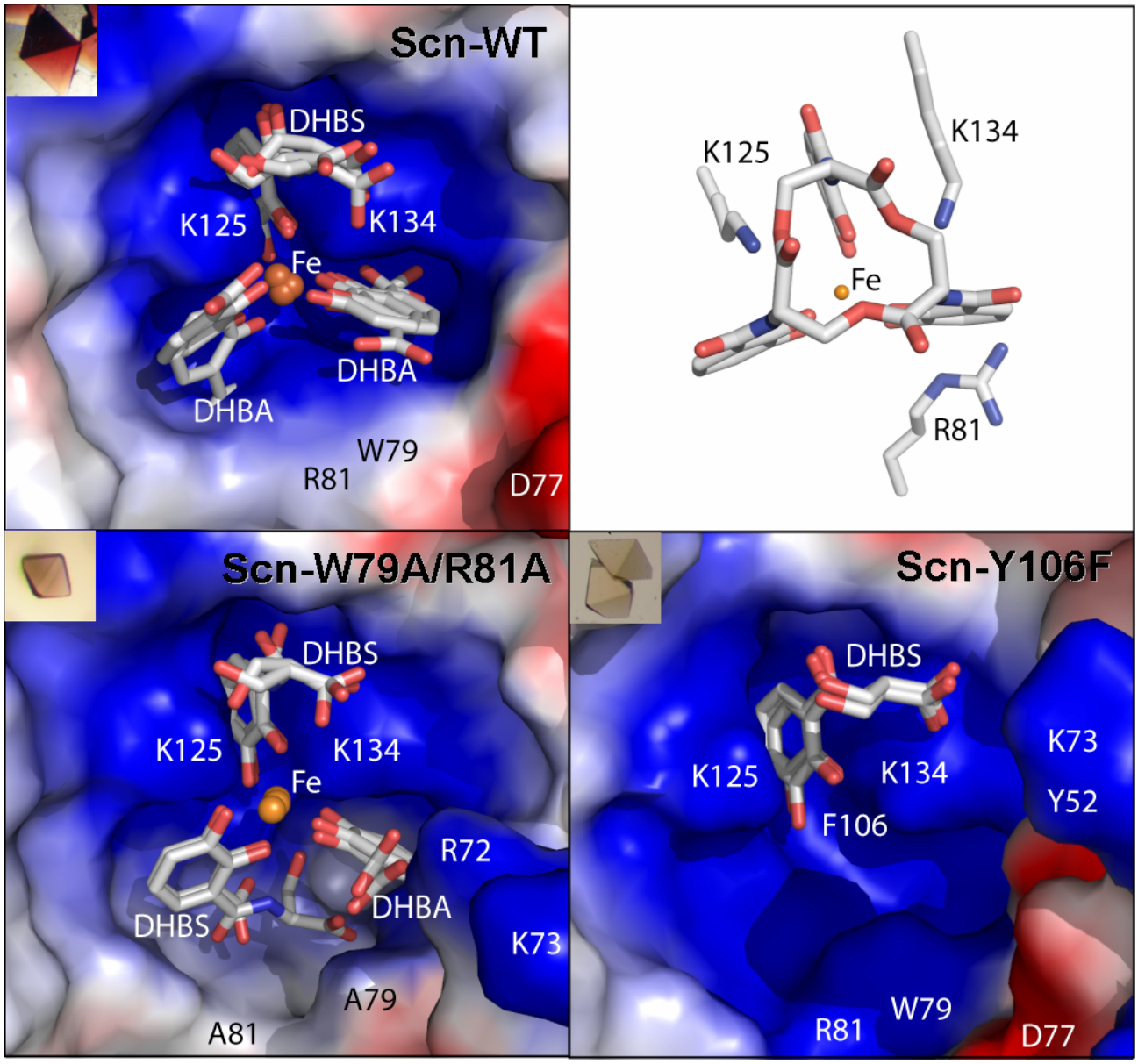

Figure 5. Removal of the steric clashes in Scn causes changes in the observed siderophore binding. Although $[Fe^{III}(Ent)]^{3-}$ is broken down in the wild type structure (top left panel) the break down products arrange themselves similar to that of the modeled intact complex (top right panel). In the Scn-W79A/R81A structure, removal of the key residues W79 and R81 allows for the binding of 2,3-DHBS in an inverted orientation (bottom left panel). In the Scn-Y106F structure, only one 2,3-DHBS fragment is bound (bottom right panel). The surface representation of the protein (top left and bottom panels) shows the electrostatic potentials for the surface of the protein (blue positively charged, white neutral, and red negatively charged). *Inserts*: co-crystals of the corresponding protein:ferric-siderophore adducts (colored for Scn and Scn-W79A/R81A; colorless for Scn-Y106F).

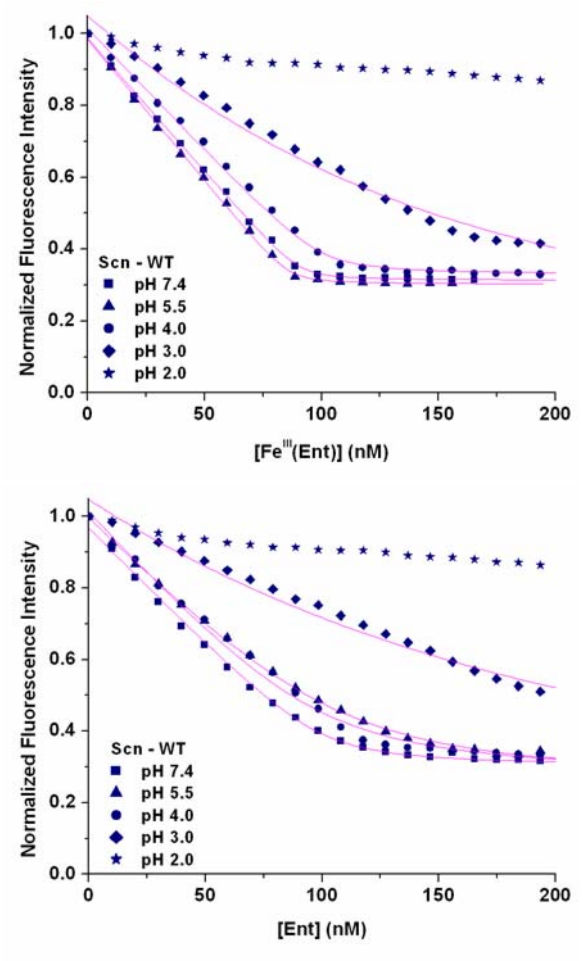

Figure 6. Fluorescence quenching analyses of wild type Scn (Scn-WT) binding with ferric- (top) and apo- (bottom) enterobactin as a function of pH. Symbols give the fluorescence data at 340 nm, and lines give the calculated fits to a one-binding site model.

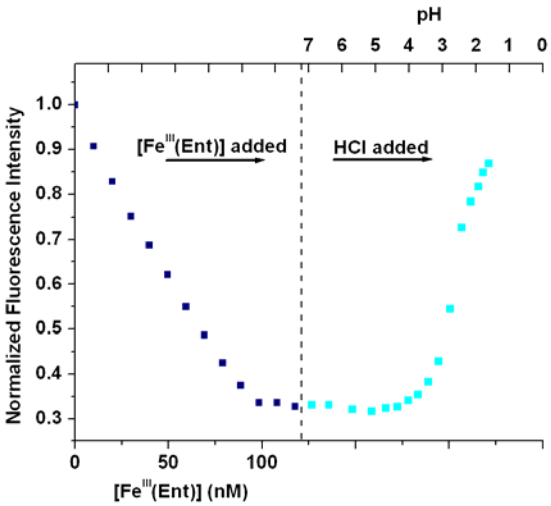

Figure 7. Fluorescence pH-titration of Scn:$[Fe^{III}(Ent)]^{3-}$. The protein fluorescence (340 nm) is first quenched by addition of ligand and increases upon acidification.

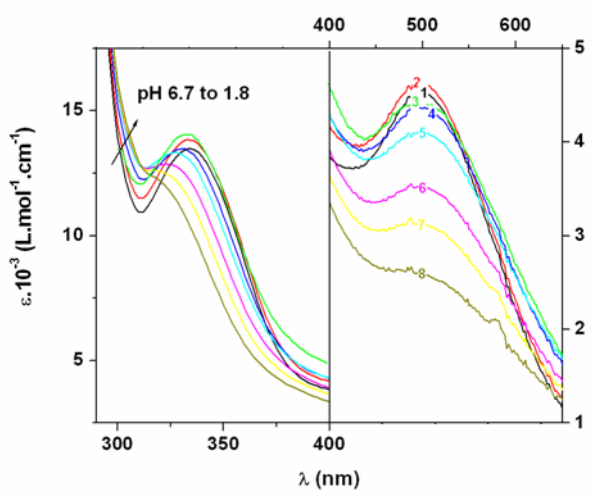

Figure 8. Spectrophotometric titration of Scn:$[Fe^{III}(Ent)]^{3-}$ by HCl in water. I = 0.1 (KCl), T = 25.0 °C, l = 1 cm. Spectra are corrected for dilution, approximately 50% of the data is shown for clarity; 1 (pH 6.68); 2 (pH 6.12); 3 (pH 5.27); 4 (pH 4.08); 5 (pH 3.58); 6 (pH 2.70); 7 (pH 2.23); 8 (pH 1.84).

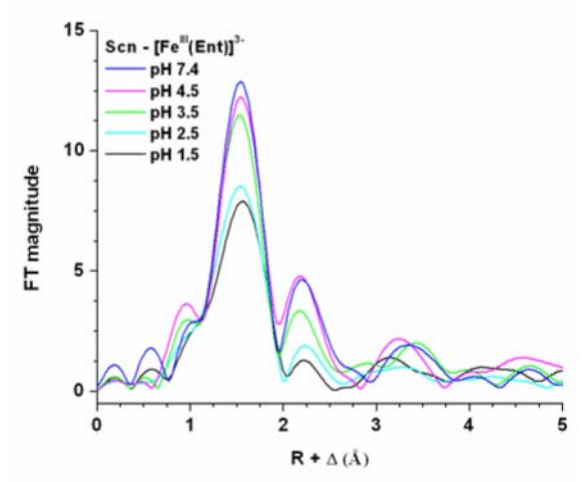

Figure 9. Fourier transforms of Scn-bound $[Fe^{III}(Ent)]^{3-}$ at pH values from 7.4 to 1.5.

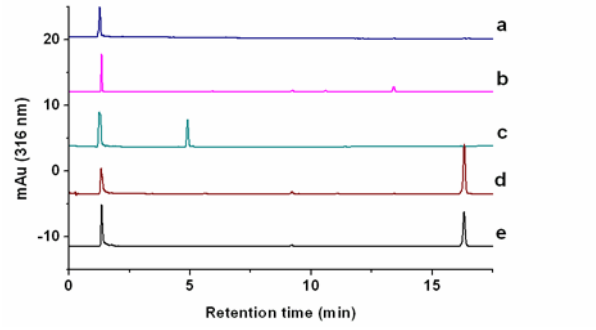

Figure 10. HPLC traces of sample solution filtrates after pH adjustment and ultracentrifugation through 10,000 kDa cutoff filters: Scn at pH 7.4 (a), Scn:$[Fe^{III}(Ent)]^{3-}$ at pH 7.4 (b), Scn:$[Fe^{III}(Ent)]^{3-}$ at pH 2.5 (c), $[Fe^{III}(Ent)]^{3-}$ at pH 7.4 (d), $[Fe^{III}(Ent)]^{3-}$ at pH 2.5 (e). The following retention times correspond to: 1.4 min, injection peak; 4.9 min, 2,3-DHBS; 16.3 min, Ent.

K_d (μM) for the equilibrium with $[Fe^{III}(Ent)]^{3-}$					
Recombinant protein	pH 7.4	pH 5.5	pH 4.0	pH 3.0	pH 2.0
Scn	0.00041 ± 0.00011	0.00015 ± 0.00003	0.00027 ± 0.00006	0.086 ± 0.001	ND
Scn-W79A/R81A	0.071 ± 0.002	0.065 ± 0.001	0.080 ± 0.020	ND	ND
Scn-Y106F	0.020 ± 0.008	0.012 ± 0.003	0.030 ± 0.001	ND	ND

K_d (μM) for the equilibrium with apo-(Ent)					
Recombinant protein	pH 7.4	pH 5.5	pH 4.0	pH 3.0	pH 2.0
Scn	0.0036 ± 0.0001	0.0055 ± 0.0024	0.011 ± 0.003	0.15 ± 0.01	ND
Scn-W79A/R81A	0.099 ± 0.005	0.11 ± 0.01	0.15 ± 0.02	ND	ND
Scn-Y106F	0.0096 ± 0.0009	0.062 ± 0.009	0.078 ± 0.016	ND	ND

Table 1. K_d values determined by fluorescence quenching for the different Scn adducts.[a,b]

[a]Uncertainties were determined from the standard deviation of at least two independent titrations.

[b]Dissociation constants could not be determined (ND) when the fluorescence curves were not indicative of specific binding.

	Scn: $[Fe^{III}(Ent)]^{3-}$	Scn-Y106F: $[Fe^{III}(Ent)]^{3-}$	Scn-W79A/R81A: $[Fe^{III}(Ent)]^{3-}$
pK_{a1}	5.72 ± 0.02	6.39 ± 0.01	6.96 ± 0.06
pK_{a2}	4.17 ± 0.09	4.73 ± 0.02	4.67 ± 0.07
pK_{a3}	2.61 ± 0.09	2.66 ± 0.02	2.89 ± 0.07

Table 2. Protonation constants of the different Scn complexes formed with ferric enterobactin.[a]

[a]Uncertainties were determined from the standard deviation of at least two independent titrations.

Complex	CN	Fe^{III}-O_{ortho} distance (Å)	Fe^{III}-O_{meta} distance (Å)	Average Fe^{III}-O length (Å)	σ^2 (Å^2)	*R*
$[Fe^{III}(Ent)]^{3-}$ pH 7.4	6.0	1.991 ± 0.003	2.022 ± 0.003	2.01 ± 0.01	0.0032 ± 0.0003	4.4 %
Scn - $[Fe^{III}(Ent)]^{3-}$ pH 7.4	6.0	1.992 ± 0.003	2.023 ± 0.003	2.01 ± 0.01	0.0035 ± 0.00034	6.1 %
Scn - $[Fe^{III}(Ent)]^{3-}$ pH 2.5	6.0	2.010 ± 0.003	2.041 ± 0.003	2.03 ± 0.01	0.0077 ± 0.00039	22 %

Table 3. EXAFS fit results for the first-shell oxygens in samples of ferric enterobactin and adducts formed with Scn at pH 7.4 and 2.5.[a]

[a]The coordination number (CN = 6.0), the amplitude reduction factor ($S_0^2 = 1$) and energy origin (E_0 = 0.4) were fixed in each case; the *R* and Debye-Waller (σ^2) factors are averaged from all independent scans, consistently with respect to each individual sample.

References

(1) Coordination Chemistry of Microbial Iron Transport. 83. Part 82: Abergel, R. J.; Zawadzka, A. M.; Raymond, K. N. *J. Am. Chem. Soc.* **2007**, *130*, 2124-2125.
(2) Ong, S. T.; Ho, J. Z. S.; Ho, B.; Ding, J. L. *Immunobiol.* **2006**, *211*, 295-314.
(3) Jurado, R. L. *Clin. Infect. Dis.* **1997**, *25*, 888-895.
(4) Devireddy, L. R.; Teodoro, L. R.; Richard, F. A.; Green, M. R. *Science* **2001**, *293*, 829-834.
(5) Flo, T. H.; Smith, K. D.; Sato, S.; Rodriguez, D. J.; Holmes, M. A.; Strong, R. K.; Akira, S.; Aderem, A. *Nature* **2004**, *432*, 917-921.
(6) Goetz, D. H.; Holmes, M. A.; Borregaard, N.; Bluhm, M. E.; Raymond, K. N.; Strong, R. K. *Mol. Cell* **2002**, *10*, 1033-1043.
(7) Fischbach, M. A.; Lin, H.; Zhou, L.; Yu, Y.; Abergel, R. J.; Liu, D. R.; Raymond, K. N.; Wanner, B. L.; Strong, R. K.; Walsh, C. T.; Aderem, A.; Smith, K. D. *Proc. Natl. Acad. Sci. USA* **2006**, *103*, 16502-16507.
(8) Fischbach, M. A.; Lin, H. N.; Liu, D. R.; Walsh, C. T. *Nature Chem. Biol.* **2006**, *2*, 132-138.
(9) Abergel, R. J.; Wilson, M. K.; Arceneaux, J. E. L.; Hoette, T. M.; Strong, R. K.; Byers, B. R.; Raymond, K. N. *Proc. Natl. Acad. Sci. USA* **2006**, *103*, 18499-18503.
(10) Annamalai, R.; Jin, B.; Cao, Z. H.; Newton, S. M. C.; Klebba, P. E. *J. Bacteriol.* **2004**, *186*, 3578-3589.
(11) Yang, J.; Mori, K.; Li, J. Y.; Barasch, J. *Am. J. Phys. Renal Phys.* **2003**, *285*, F9-F18.
(12) Yang, J.; Goetz, D. H.; Li, J. Y.; Wang, W.; Mori, K.; Setlik, D.; Du, T.; Erdjument-Bromage, H.; Tempst, P.; Strong, R. K.; Barasch, J. *Mol. Cell* **2002**, *10*, 1045-1056.
(13) Kaplan, J. *Cell* **2002**, *111*, 603-606.
(14) Devireddy, L. R.; Gazin, C.; Zhu, X.; Green, M. R. *Cell* **2005**, *123*, 1293-1305.
(15) Richardson, D. R. *Cell* **2005**, *123*, 1175-1177.
(16) Schmidt-Ott, K. M.; Mori, K.; Li, J. Y.; Kalandadze, A.; Cohen, D. J.; Devarajan, P.; Barasch, J. *J. Am. Soc. Nephrol.* **2007**, *18*, 407-413.
(17) Borregaard, N.; Cowland, J. B. *BioMetals* **2006**, *19*, 211-215.
(18) Mori, K. *et al. J. Clin. Invest.* **2005**, *115*, 610-621.
(19) Schmidt-Ott, K. M.; Mori, K.; Kalandadze, A.; Li, J. Y.; Paragas, N.; Nicholas, T.; Devarajan, P.; Barasch, J. *Curr. Opin. Nephr. Hypert.* **2006**, *15*, 442-449.
(20) Gasymov, O. K.; Abduragimov, A. R.; Yusifov, T. N.; Glasgow, B. J. *Biochemistry* **2004**, *43*, 12894-12904.
(21) Goetz, D. H.; Willie, S. T.; Armen, R. S.; Bratt, T.; Borregaard, N.; Strong, R. K. *Biochemistry* **2000**, *39*, 1935-1941.
(22) Cohen, S. M.; Raymond, K. N. *Inorg. Chem.* **2000**, *39*, 3624-3631.
(23) Abergel, R. J.; Warner, J. A.; Shuh, D. K.; Raymond, K. N. *J. Am. Chem. Soc.* **2006**, *128*, 8920-8931.
(24) Loomis, L. D.; Raymond, K. N. *Inorg. Chem.* **1991**, *30*, 906-911.
(25) Patel, R. C.; Lange, D.; McConathy, W. J.; Patel, Y. C.; Patel, S. C. *Protein Eng.* **1997**, *10*, 621-625.
(26) Holmes, M. A.; Paulsene, W.; Jide, X.; Ratledge, C.; Strong, R. K. *Structure* **2005**, *13*, 29-41.
(27) Lin, H.; Fischbach, M. A.; Liu, D. R.; Walsh, C. T. *J. Am. Chem. Soc.* **2005**, *127*, 11075-11084.
(28) Karpishin, T. B.; Dewey, T. M.; Raymond, K. N. *J. Am. Chem. Soc.* **1993**, *115*, 1842-1851.
(29) Ganz, T. *Blood* **2003**, *102*, 783-788.
(30) Nemeth, E.; Tuttle, M. S.; Powelson, J.; Vaughn, M. B.; Donovan, A.; Ward, D. M.; Ganz, T.; Kaplan, J. *Science* **2004**, *306*, 2090-2093.
(31) Cooper, S. R.; McArdle, J. V.; Raymond, K. N. *Proc. Natl. Acad. Sci. USA* **1978**, *75*, 3551-3554.
(32) Scheiber, B.; Goldenberg, H. *Arch. Biochem. Biophys.* **1993**, *305*, 225-230.

(33) Tabuchi, M.; Yoshimori, T.; Yamaguchi, K.; Yoshida, T.; Kishi, F. *J. Biol. Chem.* **2000**, *275*, 22220-22228.
(34) Ponka, P. *Kidney Int* **1999**, *55*, S2-S11.
(35) Hvidberg, V.; Jacobsen, C.; Strong, R. K.; Cowland, J. B.; Moestrup, S. K.; Borregaard, N. *FEBS lett* **2005**, *579*, 773-777.
(36) Gans, P.; O'Sullivan, B. *Talanta* **2000**, *51*, 33-37.
(37) Bundgaard, J. R.; Sengelov, H.; Borregaard, N.; Kjeldsen, L. *Biochem. Biophys. Res. Comm.* **1994**, *202*, 1468-1475.
(38) Breustedt, D. A.; Schonfeld, D. L.; Skerra, A. *Biochim. Biophys. Acta Prot. Proteom.* **2006**, *1764*, 161-173.
(39) Kuzmic, P. *Anal. Biochem.* **1996**, *237*, 260-273.
(40) Welcher, F. J. *The Analytical Uses of Ethylenediamine Tetraacetic Acid*; D. van Nostrand Co.: Princeton, NJ, 1958.
(41) Bailey, S. *Acta Crys. D* **1994**, *50*, 760-763.
(42) Otwinowski, Z.; Minor, W. In *Macromolecular Crystallography, Pt A* 1997; Vol. 276, p 307-326.
(43) Emsley, P.; Cowtan, K. *Acta Crys. D* **2004**, *60*, 2126-2132.
(44) Murshudov, G. N.; Vagin, A. A.; Dodson, E. J. *Acta Crys. D* **1997**, *53*, 240-255.
(45) Cohen, S. M.; O'Sullivan, B.; Raymond, K. N. *Inorg. Chem.* **2000**, *39*, 4339-4346.
(46) Johnson, A. R.; O'Sullivan, B.; Raymond, K. N. *Inorg. Chem.* **2000**, *39*, 2652-2660.
(47) Xu, J.; O'Sullivan, B.; Raymond, K. N. *Inorg. Chem.* **2002**, *41*, 6731-6742.
(48) Wandersman, C.; Delepaire, P. *Annu. Rev. Microbiol.* **2004**, *58*, 611-647.
(49) Gans, P.; Sabatini, A.; Vacca, A. *Ann. Chim. (Rome)* **1999**, *89*, 45-49.
(50) Ravel, B.; Newville, M. *J. Synchrotron. Rad.* **2005**, *12*, 537-541.